NeuroImage 272 (2023) 120081

Contents lists available at ScienceDirect

NeuroImage

journal homepage: www.elsevier.com/locate/neuroimage

Conscientiousness associated with efficiency of the salience/ventral attention network: Replication in three samples using individualized parcellation

Tyler A. Sassenberg[a,*], Philip C. Burton[a], Laetitia Mwilambwe-Tshilobo[b,c], Rex E. Jung[d], Aldo Rustichini[e], R. Nathan Spreng[f], Colin G. DeYoung[a]

[a] Department of Psychology, University of Minnesota, N616 Elliott Hall, 75 East River Parkway, Minneapolis, MN 55455, USA
[b] Department of Psychology, Princeton University, USA
[c] University of Pennsylvania, Annenberg School for Communication, USA
[d] Department of Neurosurgery, University of New Mexico, USA
[e] Department of Economics, University of Minnesota, USA
[f] Department of Neurology and Neurosurgery, McGill University, Canada

ARTICLE INFO

Keywords:
Conscientiousness
Individualized parcellation
Ventral attention network
Salience network
Efficiency

ABSTRACT

Conscientiousness, and related constructs impulsivity and self-control, have been related to structural and functional properties of regions in the prefrontal cortex (PFC) and anterior insula. Network-based conceptions of brain function suggest that these regions belong to a single large-scale network, labeled the salience/ventral attention network (SVAN). The current study tested associations between conscientiousness and resting-state functional connectivity in this network using two community samples (*N's* = 244 and 239) and data from the Human Connectome Project (*N* = 1000). Individualized parcellation was used to improve functional localization accuracy and facilitate replication. Functional connectivity was measured using an index of network efficiency, a graph theoretical measure quantifying the capacity for parallel information transfer within a network. Efficiency of a set of parcels in the SVAN was significantly associated with conscientiousness in all samples. Findings are consistent with a theory of conscientiousness as a function of variation in neural networks underlying effective prioritization of goals.

Within the Five Factor Model of personality, conscientiousness describes the shared variance among traits reflecting tendencies to follow rules and prioritize non-immediate goals (DeYoung, 2015). Individuals scoring high in conscientiousness are inclined toward fastidiousness, hard work, future planning, and are skilled at self-regulating and avoiding impulsivity. Conscientiousness predicts various influential life outcomes, including health-promoting behaviors, longevity, quality of familial and intergenerational relationships, academic success, workplace performance, and career success (Ozer and Benet-Martinez, 2006; Roberts et al., 2014). In predicting career and academic outcomes, it is second only to intelligence (Wilmot and Ones, 2019; Higgins et al., 2007). Further, conscientiousness represents the opposite pole of the dimension of psychopathology known as disinhibition, which is associated with externalizing problems such as attention deficit/hyperactivity disorder (ADHD) and substance use disorders (Widiger et al., 2019). Despite the clear importance of conscientiousness for human life, relatively little is established regarding its underlying neural substrate (DeYoung et al., 2021).

Based on the existing research on neural correlates of conscientiousness and impulsivity, Allen and DeYoung (2017) theorized that conscientiousness is, in part, a function of a particular broad neural network that has been identified in large studies of functional connectivity (Schaefer et al., 2018; Uddin et al., 2019; Yeo et al., 2011). This network includes core neuroanatomical regions, the anterior insula and dorsal anterior cingulate cortex (dACC), and has been studied under the labels of "salience," "ventral attention," and "cingulo-opercular" networks (Dosenbach et al., 2007; Fox et al., 2006; Seeley et al., 2007; Uddin et al., 2019). Here we refer to it as the salience/ventral attention network (SVAN). Considering the known functional properties of these networks, Rueter et al. (2018) suggested that, as a whole, the SVAN might be considered a goal priority network, responsible for prioritizing goals effectively given situational affordances and directing attention away from distractions and toward goal-relevant stimuli. In addition to anterior insula and dACC, the SVAN includes nodes in lateral PFC, including dorsolateral PFC, inferior parietal cortex (operculum) and temporoparietal junction (TPJ) (Yeo et al., 2011; Uddin et al., 2019).

* Corresponding author.
E-mail address: sasse025@umn.edu (T.A. Sassenberg).

https://doi.org/10.1016/j.neuroimage.2023.120081.
Received 7 June 2022; Received in revised form 21 March 2023; Accepted 31 March 2023
Available online 1 April 2023.

Rueter et al. (2018) attempted to perform the first direct test of the hypothesis that functional connectivity within the SVAN is positively associated with conscientiousness. However, limitations in their methods rendered it unclear to what extent their findings would generalize to other samples and how accurately they captured variance associated with the SVAN specifically. They used networks derived from independent components analysis (ICA) that did not align perfectly with the borders of the SVAN found in standard atlases. Additionally, ICA solutions are unique to the sample in which the ICA was conducted, which impedes replication. In the present research, we rely on the atlases of Yeo et al. (2011) and Schaefer et al. (2018) to define the SVAN. This allowed us to test the SVAN hypothesis and to reproducibly assess the same functional neuroanatomy across multiple samples.

A major challenge when testing hypotheses regarding individual differences in networks from standard atlases is that these networks are not in the same spatial locations for everyone, relative to anatomical landmarks (Chong et al., 2017; Gordon et al., 2017; Kong et al., 2018). Thus, if one overlays a standard network atlas on each individual's structurally aligned data, the boundaries will be poorly estimated for everyone. To better estimate regional boundaries, those boundaries must be adjusted for each subject. To accomplish that adjustment, we employed a relatively new technique to accomplish the individualization of network locations based on an iterative Bayesian process known as group prior individualized parcellation (GPIP; Chong et al. 2017). In GPIP (and similar procedures, e.g., Kong et al. 2021), one begins with the boundaries of a standard atlas of distributed networks or smaller contiguous parcels. Then, patterns of covariance in fMRI data for each subject are used to adjust the boundaries of the atlas to optimize them to that subject's unique functional connectivity pattern. Thus, all networks and parcels are present in each subject and retain their group label across subjects, but their size, shape, and location are individualized.

Individualized parcellation inherently produces greater within-parcel covariance, and this seems to be a good marker of true functional coherence. Compared to non-individualized atlases, individualized parcellations correspond better to regions of task-related activation, which conform more closely to functional organization than to anatomical location (Chong et al., 2017). It also improves prediction of a wide range of individual differences (Anderson et al., 2021; Kong et al., 2021; Setton et al., 2022). Coupled with the fact that individual parcels from standard atlases can easily be compared across subjects and samples, these findings suggest that individualized parcellation should become standard practice in neuroimaging research on individual differences (DeYoung et al., 2022).

We tested the theorized association of conscientiousness with connectivity in the SVAN, using this approach in the original sample studied by Rueter et al. (2018) as well as two additional independent samples, including data from the Human Connectome Project (HCP). We used an atlas by Schaefer et al. (2018) with 400 parcels which aligns very closely with the canonical networks identified by Yeo et al. (2011). Our hypothesis was that functional connectivity among parcels in the SVAN would be positively associated with conscientiousness. We quantified functional connectivity using a measure of network efficiency that reflects the capacity for parallel information transfer within a network and that has been identified as a reliable metric for characterizing functional network integration (Bullmore and Sporns, 2012; Deuker et al., 2009; Jiang et al., 2021). To avoid assuming that every parcel in the network must be equally important to conscientiousness, we also examined subsets of parcels within the SVAN and its subnetworks.

1. Methods

1.1. Sample 1

1.1.1. Participants

A total of 306 right-handed participants completed a single resting-state fMRI session as part of a larger study. Participants were recruited through online advertisements and fliers posted in public areas in the metro region around Minneapolis and St. Paul, Minnesota. Exclusion criteria included fMRI contraindications, a diagnosis of neurological or severe psychiatric conditions, or substantial behavioral dysfunction attributable to drug or alcohol use. Following recruitment, additional participants were excluded due to incomplete or poor quality fMRI data, incomplete behavioral data, poor FreeSurfer surface alignment, and excessive head movement during the scan, as identified through multiple data preprocessing pipelines applied in subsequent analyses. A total of 244 subjects were retained (121 females) ranging from 20 to 40 years old ($M = 25.9$, $SD = 4.7$). Protocols used in this study were approved by the University of Minnesota Twin Cities institutional review board, and all participants provided written informed consent.

1.1.2. Personality measures

Participants in the present study completed two personality questionnaires, the Big Five Aspect Scales (BFAS; DeYoung et al. 2007) and the Big Five Inventory (BFI; John et al. 2008). The BFAS comprises 100 items on a 5-point Likert scale ranging from 1 (*strongly disagree*) to 5 (*strongly agree*). The questionnaire measures two lower-order aspects for each of the Big Five, with 10 items per aspect. These aspect scores can be averaged to create 20-item domain level Big Five scores. The BFI consists of a total of 44 items measuring domain level Big Five factors on a 5-point Likert scale ranging from 1 (*strongly disagree*) to 5 (*strongly agree*). In addition to self-report measures, peer-report measures were obtained by providing participants with 3 packets with instructions to have both questionnaires completed by individuals who knew the participant well. At least one peer report was available for 182 participants, and multiple peer-reports for a given subject were averaged to create a single peer-report score, when applicable. Scale scores for Conscientiousness across the BFAS and BFI were averaged to create a composite variable, and self and peer-report measures were averaged when applicable.

1.1.3. Intelligence

All participants completed a subset of the Wechsler Adult Intelligence Scale – Fourth Edition (WAIS-IV; Wechsler 2008), the Block Design, Matrix Reasoning, Vocabulary, and Similarities tests. Although the present study selected these tests from the full WAIS-IV, these four tests are identical to those used in the shorter alternative, the Wechsler Abbreviated Scale of Intelligence (WASI), and provide reliable estimates of full-scale IQ (Wechsler, 2011).

1.1.4. fMRI data acquisition and preprocessing

fMRI data were acquired using a 3T Siemens Trio Scanner at the Center for Magnetic Resonance Research at the University of Minnesota Twin Cities. High-resolution T1-weighted MPRAGE images with the following parameters were acquired for anatomical surface registration for each participant: voxel dimensions = $1 \times 1 \times 1$ mm^3; repetition time (TR) = 1.9 s; echo time (TE) = 0.29 ms; flip angle = 9°. Functional echo-planar images were acquired with the following parameters: 35 coronal slices; TR = 2 s; TE = 28 ms; flip angle = 80°; voxel dimensions = $3.5 \times 3.5 \times 3.5$ mm.

Results included in this study come from preprocessing performed using *fMRIPrep* version 20.2.1 (Esteban et al., 2018). Details of the full *fMRIPrep* analysis are reported in the supplementary material. In short, T1-weighted images were processed through the recon-all function from Freesurfer v6.0.1, and were also nonlinearly spatially normalized to MNI152NLin6Asym space using ANTs v2.1.0. Resting-state scans were corrected for field-map distortions, rigidly coregistered to T1 native space, motion corrected, and also normalized to standard space. ICA-AROMA was used to generate a non-aggressively denoised variant of the data. Anatomical CompCor was run and the top five principal components of both CSF and white matter were retained. Preprocessed functional data in T1 native space were used for subsequent analyses, and were visually inspected after coregistration to ensure high-quality data was included. Participants exhibiting a relative mean framewise

displacement greater than 0.5 mm, a mean standardized derivative of RMS variance over voxels (DVARS) greater than 1.5, or any single occurrence of a coordinate displacement greater than 2.75 mm were excluded from subsequent analyses to avoid biased effects in associations with measures of functional connectivity (Power et al., 2012, 2014).

1.2. Sample 2

1.2.1. Participants

A total of 260 participants were recruited through postings throughout the University of New Mexico, nearby high schools, and various professional STEM businesses from communities surrounding Albuquerque, New Mexico. Participants were excluded on the basis of neurological and psychological disorders, fMRI contraindications, incomplete behavioral data, incidental fMRI findings, poor FreeSurfer surface registration, and excessive head motion identified through data preprocessing. A total of 239 participants were retained for the present study (117 females) ranging from 16 to 38 years old (M = 22, SD = 3.9). All participants provided written informed consent, and all procedures in this study were approved by the University of New Mexico institutional review board.

1.2.2. Personality measures

All participants included in the present study completed one of two personality questionnaires: the BFAS, or the NEO Five-Factor Inventory (FFI). The NEO-FFI represents a subset of the full NEO Personality Inventory, Revised (NEO PI-R; Costa and McCrae 1992), consisting of 12 items per factor. Scale scores were calculated as item averages, using a five-point Likert scale ranging from 0 (*strongly disagree*) to 4 (*strongly agree*). A total of 59 participants completed the NEO-FFI, and 180 participants completed the BFAS. To account for differences in scale means, scores were centered by subtracting the sample mean of their respective scale. The present study utilized Conscientiousness scores from all participants.

1.2.3. Intelligence

All participants were administered the set of four tasks from the WASI (Wechsler, 2011). Full-scale IQ was estimated from performance on the Vocabulary, Similarities, Matrix Reasoning, and Block Design subtests.

1.2.4. fMRI data acquisition and preprocessing

Using a 3T Siemens Prisma scanner, resting-state functional echo-planar images were acquired with the following parameters: 32 coronal slices; TR = 275 ms; TE = 30 ms; flip angle = 34°; multiband acceleration factor = 8; voxel dimensions = 3.5 × 3.5 × 3.5 mm, pixel bandwidth = 1736 Hz. High-resolution T1-weighted MPRAGE images were acquired for anatomical surface registration through a 5 echo sequence with the following parameters: TR = 25.3 s; TE = 1.64 ms, 3.5 ms, 5.36 ms, 7.22 ms, 9.08 ms; flip angle = 7°; voxel dimensions = 1 × 1 × 1 mm^3. Results included in this study come from preprocessing performed using *fMRIPrep* version 20.2.1 using the same specifications described for Sample 1.

1.3. Sample 3

1.3.1. Participants

A total of 1000 participants (533 females) were selected from the WU-Minn Consortium of the Human Connectome Project (Van Essen et al., 2012). Participants were initially excluded on the basis of a history of severe psychiatric, neurological, or medical disorders. Among the participants of the 1200 young adult sample, additional participants were excluded due to missing personality and intelligence task data, and missing resting-state fMRI scan data. Participants' ages ranged from 22 to 37 years old (M = 28.7, SD = 3.7). All participants provided informed consent, and all study protocols were approved by the Institutional Review Board of Washington University in St. Louis. Details of the informed consent procedure are provided by Van Essen et al. (2013).

1.3.2. Personality measures

Participants completed the NEO-FFI to assess trait Conscientiousness. Scale scores were assessed using a five-point Likert scale ranging from 0 (*strongly disagree*) to 4 (*strongly agree*).

1.3.3. Intelligence

Intelligence was assessed as a composite of performance measures from a set of three tests from the NIH Toolbox (Heaton et al., 2014) and Penn Computerized Neurocognitive Battery (Moore et al., 2015). Performance metrics on the Matrix Reasoning, Picture Vocabulary, and List Sorting tasks were averaged to create an estimate of intelligence for analyses.

1.3.4. fMRI data acquisition and preprocessing

fMRI data were acquired using a customized 3T Siemens Skyra scanner for all participants at Washington University in St. Louis. The present study used a single left-to-right phase encoded resting-state scan acquired using the following parameters: 72 axial slices; TR = 0.4 s; TE = 33 ms; flip angle = 52°; multiband acceleration factor = 8; voxel dimensions = 2 × 2 × 2 mm^3; pixel bandwidth = 2290 Hz. Additionally, high-resolution T1-weighted MPRAGE structural images were acquired for anatomical surface registration with the following parameters: TR = 24 s; TE = 2.14 ms; flip angle = 8°; voxel dimensions = 0.7 × 0.7 × 0.7 mm^3. Resting-state scans were preprocessed using the HCP minimal preprocessing pipeline and motion artifacts were removed using ICA-FIX (Burgess et al., 2016). Relative mean framewise displacement was also computed to be included as a covariate in subsequent analyses. Features of the HCP minimal preprocessing pipeline are described in greater detail in previous literature (Glasser et al., 2013; Ugurbil et al., 2013).

1.4. Group prior individualized parcellation

Functional connectivity networks were identified using an individualized cortical parcellation approach. For participants in all three samples, ICA-denoised resting-state fMRI scans in subject-native space were first resampled to a common cortical surface mesh (Dale et al., 1999), and the BOLD timeseries at each vertex was normalized to zero mean and unit variance. The resulting subject surface data were then initialized using a pre-defined group atlas with 400 functionally distinct regions (Schaefer et al., 2018) mapped to the 17-network atlas defined by Yeo et al. (2011). This 400 parcel atlas was used to balance the tradeoff between identifying broad patterns of functional connectivity corresponding to the networks defined by Yeo et al. (2011) while also identifying smaller-resolution functional regions that may be informative in identifying individual differences in functional connectivity. A Bayesian algorithm was applied to iteratively adjust parcel boundaries according to each participant's unique patterns of functional connectivity (Chong et al., 2017; Setton et al., 2023). In order to produce stable modifications of parcel boundaries, this algorithm utilized 20 iterations to maximize within-parcel homogeneity and ensure that all participants had no more than one vertex changing its parcel label on the final iteration. Through this process, each participant acquired a unique modification of a standard group-level atlas after the final iteration such that the boundaries of the parcels of the initial atlas optimally reflected each individual's patterns of resting-state functional connectivity.

For the present analyses, the full SVAN was defined by 51 functional parcels, 34 of which correspond to subnetwork A, and 17 of which correspond to subnetwork B, in the 17-network atlas of Yeo et al. (2011). The full SVAN was included in the present analyses to account for the potential role of connections between parcels of subnetworks A and B, rather than focusing only connections within each subnetwork separately. (The two subnetworks fractionate the larger network labeled "ventral attention network" in Yeo et al. 2011 7-network atlas.) The parcels of the SVAN are illustrated using the group-level Schaefer atlas (Schaefer et al., 2018) in Fig. 1. Analyses of the extent of the spatial modification of the

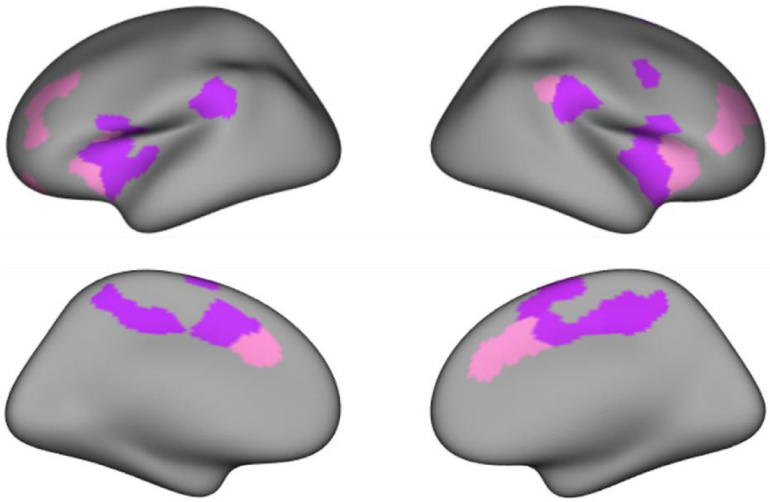

Fig. 1. Parcels in the salience/ventral attention network (SVAN). Colors correspond to 2 of the 17 functional networks described by Yeo et al. (2011). Purple = SVAN subnetwork A, Pink = SVAN subnetwork B.

SVAN and its subnetworks through GPIP are described in the supplementary material.

1.5. Orthogonal minimum spanning trees and functional connectivity

For each sample, parcel-average timeseries were correlated and Fisher r-to-z transformed to create a 400 × 400 functional connectivity matrix for each participant. Using these matrices, smaller sub-matrices were constructed for correlations among parcels in the SVAN, subnetwork A, and subnetwork B. To quantify the connectivity properties of each matrix, a graph-theory approach was used, in which each parcel is considered a node in the graph and each correlation represents a potential connection, or edge, between nodes.

We applied a data-driven topological threshold to the individual functional connectivity matrices using orthogonal minimum spanning trees (OMSTs; Dimitriadis et al. 2017). The OMSTs approach was used to screen out many low correlations and avoid modeling noise that may be present in functional connectivity measures, while also avoiding the imposition of arbitrary graph thresholds that incur methodological biases. OMSTs rely on an iterative procedure to filter functional connectivity networks to optimize the trade-off between global efficiency within the network and the wiring cost, where global efficiency describes the average inverse shortest path length within the network, and wiring cost refers to the ratio of the sum of the weights of the filtered graph to that of the unfiltered graph (Rubinov and Sporns, 2010). In this manner, connections between participants' OMSTs using an identical set of nodes can vary substantially on account of unique individuals' patterns of brain organization, while still ensuring a fully connected graph, a property generally exhibited by unfiltered weighted graphs. We emphasize the importance of utilizing a fully connected graph for each network of interest to reflect that these parcels demonstrate functional interactions within canonical networks described by the group-level cortical atlas. Despite the application of a degree of sparsity to the functional connectivity matrices using OMSTs, this thresholding procedure has been demonstrated to produce (1) graphs characterized by similar sensitivity to perturbations in connection strength and density compared to unfiltered graphs (Tewarie et al., 2015), (2) higher performance compared to conventionally filtered graphs in tests of subject-specific graph recognition (Dimitriadis et al., 2017), and (3) greater test-retest reliability across scans compared to graphs with conventional thresholds (Jiang et al., 2021).

We computed a measure of global-cost efficiency of OMSTs-filtered graphs as an index of network-wide functional connectivity. In the present analyses, global-cost efficiency reflects coherence among sets of parcels as a function of correlations between average parcel timeseries in the filtered graph. The choice of this particular graph theoretical measure is informed by research demonstrating its reliability as a measure of functional network integration (Bullmore and Sporns, 2012; Deuker et al., 2009; Jiang et al., 2021). In the present research, "global" does not refer to the set of nodes spanning the entire cortex, but rather to the full set of nodes in any network or subnetwork of interest. To avoid confusion, we will hereafter refer to this metric as "network efficiency."

1.6. Analysis

We used two main analytic strategies. First, we examined associations between conscientiousness and network efficiency among all parcels within each network of interest. Second, we applied a permutation-based feature selection approach to identify potentially relevant subsets of parcels within each network. This approach was used to address the possibility that only a subset of parcels within the SVAN might be important for conscientiousness, and to mitigate the potential influence of intraindividual noise in pairwise functional connectivity among many parcels. This approach is inspired by the data-driven, machine-learning method called Connectome-Based Predictive Modeling (CPM; Finn et al. 2015). CPM uses cross-validation to identify unique brain-behavior associations using functional connectivity data and has been effective in identifying significant and reliable associations across large samples (Rosenberg et al., 2015; Wang et al., 2021). However, since CPM is primarily a data-driven procedure, using this method across multiple samples introduces the likely possibility of identifying different configurations of edges in each, which is not suitable for the goal of identifying replicable groups of parcels. To take advantage of CPM's capacity to summarize broad patterns of functional connectivity, we used a variation of the feature selection criteria described in the CPM procedure to identify a single set of parcels whose associations with conscientiousness could be tested across multiple samples.

For tests of associations between conscientiousness and subsets of the networks of interest (i.e., SVAN and its subnetworks A and B), we randomly divided participants in each sample into ten equal sized subgroups. Using nine of the ten subgroups, partial correlations were computed between each edge in OMSTs-filtered functional connectivity matrices and conscientiousness, controlling for the effects of head motion using relative mean framewise displacement. This procedure was repeated ten times, holding out each subgroup once. In each iteration, a binarized matrix of the graph was created denoting edges positively associated with conscientiousness at $p < .05$ (uncorrected). These p-values remained uncorrected because we were using them merely as a convenient threshold for identifying parcels to include in larger networks of interest, and they were not used as inferential statistics to test our main hypothesis. Across the ten iterations, these matrices were combined to represent the frequency of iterations in which edges demon-

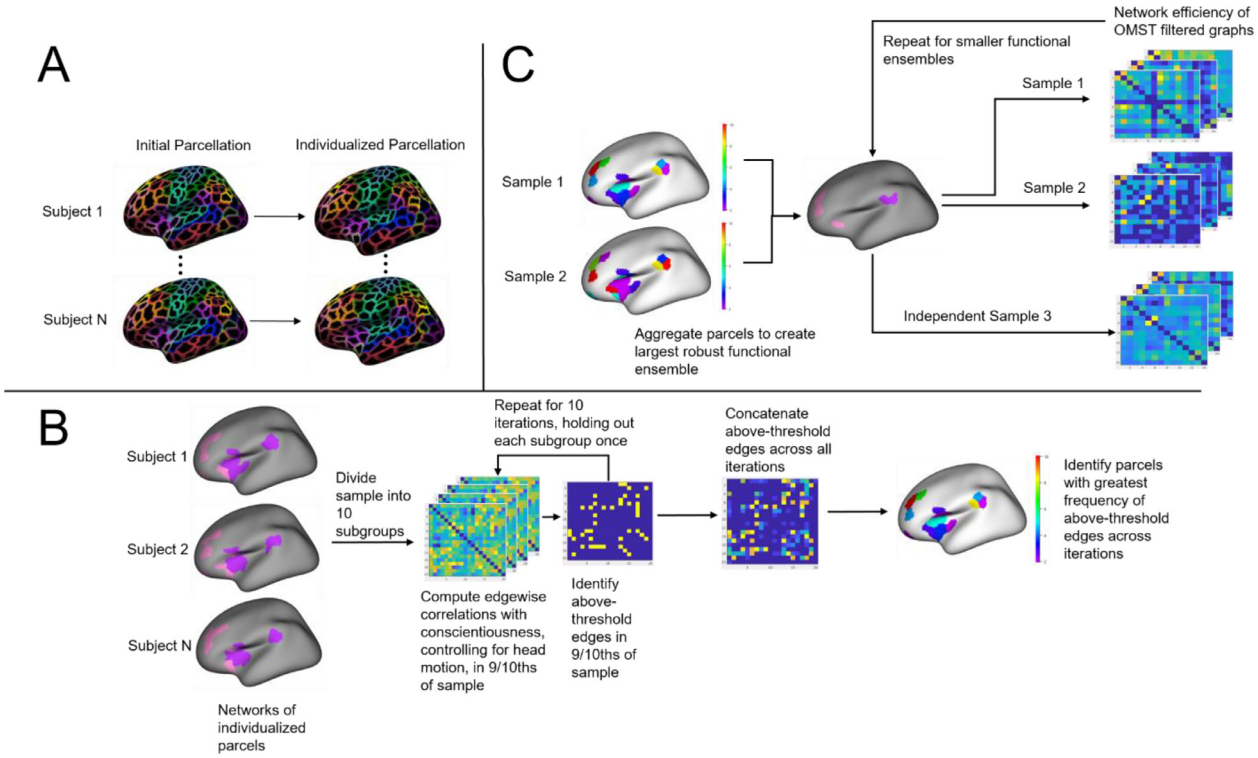

Fig. 2. Workflow of method for identifying functional ensembles in each sample. Panel **A:** GPIP was used to individualize the locations and boundaries of parcels from the 400 parcel atlas by Schaefer et al. (2018). The procedure in panel **B** was used to identify a computationally feasible number of parcels for inclusion in network analyses and was conducted in all samples, but no parcels in Sample 3 met the selection criteria. Network efficiency from combinations of parcels meeting the selection criteria in Samples 1 and 2 identified in **B** was tested independently in Sample 3, as illustrated in panel **C.**

strated above-threshold associations with conscientiousness. The maximum value of each row in this matrix was used to signify the robustness to sampling variability of associations between conscientiousness and the connectivity of each parcel. For each sample, parcels were selected for further analyses if they contained an edge significantly positively associated with conscientiousness in at least 8 iterations. The division of each sample into subgroups was designed to reduce the influence of sampling variability by identifying parcels that had above-threshold associations with conscientiousness across many subsamples, in line with conventional thresholds used in CPM (Shen et al., 2017).

Although we had initially planned to identify candidate parcels in every sample, we ultimately decided to leave Sample 3 (HCP) out of any procedure for selecting parcels of interest so that we could hold out a large and completely independent sample in which to replicate our findings. Reserving the largest sample for replication allowed for the most rigorous test of the robustness of our findings. We therefore combined parcels that met the aforementioned criteria from the smaller Samples 1 and 2 to create the pool of candidate parcels for each network. This yielded 14 parcels for the SVAN, 5 parcels in subnetwork A, and 9 parcels in subnetwork B. Associations between conscientiousness and efficiency of parcels in this pool were then tested independently in Sample 3. This procedure ensured that we could replicate findings from Samples 1 and 2 in a much larger sample, with complete statistical independence from any prior analyses in that sample. This workflow is illustrated in Fig. 2.

We focused our parcel selection on edges with positive associations with conscientiousness to match the direction of our hypothesis. This procedure has the potential to engender misleading conclusions in subsequent tests of association with network efficiency because, even if some collections of parcels in the SVAN have positive associations with conscientiousness, others might show negative associations, which would be contrary to our hypothesis. To account for this possibility, we repeated our selection procedure using parcels exhibiting at least one edge with a negative association with conscientiousness in at least 8 iterations (uncorrected $p < .05$) in Samples 1 or 2. Results from this procedure are reported in the supplementary material.

Following parcel selection, we computed the set of combinations of selected parcels containing a minimum of 3 parcels each to run through the OMSTs procedure, because a network of 3 nodes is the smallest network for which more than one spanning tree exists (i.e., the smallest fully-connected network with no loops and with potential variability in the configuration of edges). Although these combinations of parcels are treated as "networks" in the graph-theory sense, we use the term "functional ensembles" to describe them from here on, to avoid confusion with our use of "network" to refer to established large-scale brain networks such as the SVAN and its two subnetworks. The largest functional ensemble for a given network of interest was defined as containing all parcels selected in the permutation procedure described above (hence 14 parcels in the SVAN, 5 parcels in subnetwork A, and 9 parcels in subnetwork B). We computed measures of network efficiency for the largest functional ensemble and for all smaller functional ensembles within each set.

Multiple linear regression models were computed predicting conscientiousness from the efficiency of each network or functional ensemble of interest, controlling for age, sex, intelligence, head motion, and efficiency of two other major neural networks (computed using OMSTs-filtered matrices in the same manner as for the SVAN), the frontoparietal control network (FPCN) and default network (DN) (Yeo et al., 2011). Network efficiency values for FPCN and DN were included as covariates for two reasons: First, these networks, like the SVAN, have extensive nodes in lateral prefrontal cortex and insula, and they have additional nodes adjacent to the SVAN throughout the brain. Given their involvement in complex cognitive functions such as working memory (FPCN) and self-generated thought (DN), one can imagine plausible functional

arguments linking them to conscientiousness that would not apply to other networks such as visual or somatomotor. Controlling for their efficiency allows a test of discriminant validity, helping to ensure that any detected associations with conscientiousness are specific to the SVAN, per our hypothesis. Second, a general tendency exists in resting-state fMRI for all brain regions and networks to exhibit positive correlations in their activity over time, which may be substantive or artifactual or some combination of both (Rueter et al., 2018). Controlling for the variance in two other large networks removes this general, possibly artifactual variance that the SVAN shares with other parts of the brain. Together, the SVAN, FPCN, and DN account for 191 of the 400 parcels in the Schaefer atlas.

Intelligence was incorporated into analyses to account for both its modest negative association with conscientiousness and its potentially confounding associations with patterns of functional connectivity in the networks relevant to our hypotheses (Cole et al., 2012; Finn et al., 2015). Leaving intelligence out of the analyses did not produce appreciable differences in our results.

All coefficients denoting the association between conscientiousness and efficiency of sets of parcels within the SVAN were corrected for Type I error ($\alpha = 0.05$) using positive false discovery rate (pFDR; Storey 2002, 2003). To evaluate the significance of each functional ensemble while accounting for the unique distributions of effect sizes in each sample, we utilized the algorithm described by Storey and Tibshirani (2003) to estimate a q-value for each functional ensemble, the pFDR analog of the p-value.

Finally, to investigate discriminant validity thoroughly, we checked whether networks and functional ensembles were consistently associated with any of the other Big Five traits. These analyses were exploratory, but we hypothesized that efficiency of the SVAN and its various subcomponents would not be consistently associated with traits other than conscientiousness.

1.7. Data/Code availability

Individual data from Sample 1 are not able to be shared through open access because participants agreed during the informed consent procedure that their data would not be shared beyond the research team. Data from Sample 3 are available from the Human Connectome Project's website: https://www.humanconnectome.org/study/hcp-young-adult. A sample-average functional connectivity matrix from Sample 1 using individualized parcels, as well as individualized functional connectivity matrices from Sample 2 are available in an Open Science Framework repository: https://osf.io/zju2s/?view_only=8521207b2af540b9bab3b04033744f39. This repository also contains scripts used in group-level analyses. Code used to produce individualized parcels is available at https://neuroimageusc.github.io/GPIP

2. Results

Descriptive statistics for personality questionnaire measures for all samples are reported in Table 1. Distributions of the personality scores are illustrated in the supplementary material.

Standardized regression coefficients from models predicting conscientiousness from efficiency of the SVAN, its subnetworks, and their largest functional ensembles are presented in Table 2. All parcels identified in the permutation selection procedure that were used to create combinations of functional ensembles for each network of interest are reported in the supplementary material.

2.1. SVAN

The efficiency of the full SVAN, containing all parcels in both subnetworks, was positively associated with conscientiousness in Sample 3, but not Samples 1 and 2. The largest functional ensemble of the SVAN was characterized by a total of 14 parcels located in regions of the left parietal operculum and dorsolateral PFC, right superior frontal gyrus and ventrolateral PFC, and bilateral dACC and insula (Fig. 3). Although the individualization of these parcels makes the correspondence between their boundaries and standard anatomical boundaries inexact, we report the anatomical names associated with each of the parcels from the group-level atlas to facilitate discussion of the approximate brain regions associated with these networks.

These names, indices from Schaefer et al. (2018) parcellation scheme (available at https://github.com/ThomasYeoLab/CBIG/blob/master/stable_projects/brain_parcellation/Schaefer2018_LocalGlobal/Parcellations/MNI/Centroid_coordinates/Schaefer2018_400Parcels_17Networks_order_FSLMNI152_1 mm.Centroid_RAS.csv), and centroid coordinates for all parcels in the largest functional ensemble of the SVAN are reported in Table 3.

The efficiency of this functional ensemble was significantly associated with conscientiousness across all samples. Additionally, conscientiousness was positively associated with all combinations of smaller functional ensembles in Sample 2. Similar associations were found in Samples 1 and 3, where conscientiousness was positively associated with 15,616 smaller functional ensembles (96% of all combinations) in Sample 1 and 11,552 smaller functional ensembles (71% of all combinations) in Sample 3, after controlling pFDR (q <0.05).

2.1.1. Subnetwork A

In tests of association with subnetwork A of the SVAN (Table 2), conscientiousness was negatively associated with the efficiency among all parcels in the full subnetwork in Sample 2. However, in Samples 1 and 2, conscientiousness was positively associated with the largest functional ensemble, containing a set of 5 parcels within the left parietal operculum, and the bilateral medial frontal and parietal cortex. Among the combinations of smaller functional ensembles derived from these 5 parcels, conscientiousness was associated with all of these functional ensembles in Sample 1 after pFDR correction for multiple comparisons, but these associations were not replicated in Samples 2 and 3.

2.1.2. Subnetwork B

In tests of association with subnetwork B of the SVAN (Table 2), conscientiousness was significantly associated with the efficiency of all parcels in Samples 1 and 2, but not in Sample 3. Additionally, conscientiousness was significantly associated with the largest functional ensemble in Samples 1 and 2. This functional ensemble contained 9 parcels dispersed throughout the left and right dorsolateral PFC, insula, and dorsomedial PFC. Among the combinations of smaller functional ensembles created using these parcels, conscientiousness was positively associated with 229 functional ensembles (49% of all combinations) in Sample 1 and 164 functional ensembles (35% of all combinations) in Sample 2, after controlling pFDR.

Table 1
Descriptive statistics for personality measures.

	M	*SD*	Skew	Kurtosis
Sample 1 (N = 244)				
Self-report BFAS Conscientiousness	3.39	.61	−0.20	−0.29
Self-report BFI Conscientiousness	3.75	.63	−0.50	.10
Peer-report BFAS Conscientiousness	3.42	.55	−0.17	−0.25
Peer-report BFI Conscientiousness	3.66	.45	−0.57	−0.12
Composite Conscientiousness	3.55	.50	−0.36	−0.07
Sample 2 (N = 239)				
BFAS Conscientiousness	3.49	.51	−0.23	−0.63
NEO-FFI Conscientiousness	2.76	.57	−0.36	.26
Sample 3 (N = 1000)				
NEO-FFI Conscientiousness	2.87	.49	−0.36	.19

Note. BFAS = Big Five Aspect Scales, BFI = Big Five Inventory, NEO-FFI = NEO Five Factor Inventory.

Table 2
Standardized regression coefficients in models predicting conscientiousness from efficiency of whole networks and largest functional ensembles of the SVAN.

Model	Sample 1 (N = 244)		Sample 2 (N = 239)		Sample 3 (N = 1000)	
	All Parcels	Largest Functional Ensemble	All Parcels	Largest Functional Ensemble	All Parcels	Largest Functional Ensemble
Conscientiousness						
SVAN	−0.01	**.24****	−0.01	**.33****	.12*	.12*
age	**.17**	**.19**	.07	.06	.04	.03
Sex (male)	**−0.45**	**−0.41**	**−0.55**	**−0.48**	**−0.17**	**−0.16**
intelligence	**−0.14**	**−0.13**	.00	−0.01	**−0.10**	**−0.10**
head motion	−0.06	−0.10	−0.04	−0.05	−0.06	−0.06
DN	.00	−0.08	.15	.04	−0.14	−0.13
FPCN	.04	−0.09	−0.09	**−0.28**	−0.03	−0.04
Conscientiousness						
Subnetwork A	.01	**.24****	−0.13*	.09*	.08	.03
age	**.17**	**.17**	.07	.07	.04	.04
Sex (male)	**−0.45**	**−0.42**	**−0.55**	**−0.54**	**−0.17**	**−0.16**
intelligence	**−0.14**	−0.12	−0.01	.00	**−0.10**	**−0.10**
head motion	−0.06	−0.10	−0.04	−0.04	−0.06	−0.06
DN	−0.01	−0.08	.18	.13	−0.12	−0.09
FPCN	.03	−0.06	−0.01	−0.15	−0.01	.01
Conscientiousness						
Subnetwork B	.21*	**.20***	.21*	.19*	.09	.04
Age	**.18**	**.18**	.07	.07	.04	.04
Sex (male)	**−0.41**	**−0.40**	**−0.52**	**−0.52**	**−0.16**	**−0.16**
Intelligence	**−0.14**	**−0.14**	−0.01	−0.01	**−0.10**	**−0.10**
Head motion	−0.10	−0.10	−0.05	−0.06	−0.05	−0.06
DN	−0.07	−0.07	.06	.07	−0.12	−0.09
FPCN	−0.08	−0.05	−0.19	−0.17	−0.03	.00

Note.
* q <0.05,
** q < 0.01 controlling for multiple comparisons across all tested functional ensembles (16,278 SVAN combinations, 16 Subnetwork A combinations, and 466 Subnetwork B combinations). Significant estimates at uncorrected p < .05 for each regression are shown in bold. SVAN = salience/ventral attention network. Largest functional ensemble refers to the set of all parcels identified by the permutation selection procedure.

Table 3
MNI152 1 mm RAS coordinates for centroids of parcels mapped to the largest functional ensemble of the SVAN.

Parcel Index	Parcel Name	R	A	S
86	LH_SalVentAttnA_ParOper_1	−55	−32	22
87	LH_SalVentAttnA_ParOper_2	−58	−44	27
98	LH_SalVentAttnA_FrMed_1	−7	0	57
99	LH_SalVentAttnA_FrMed_2	−5	9	48
101	LH_SalVentAttnB_PFCl_1	−38	49	11
102	LH_SalVentAttnB_PFCl_2	−29	43	30
105	LH_SalVentAttnB_Ins_2	−33	25	−1
288	RH_SalVentAttnA_PrC_1	51	3	41
296	RH_SalVentAttnA_FrMed_1	7	2	43
303	RH_SalVentAttnA_FrMed_4	16	7	69
305	RH_SalVentAttnB_PFClv_1	49	40	5
309	RH_SalVentAttnB_Ins_1	34	21	−8
311	RH_SalVentAttnB_PFCmp_1	8	35	25
312	RH_SalVentAttnB_PFCmp_2	7	19	35

Note. LH = left hemisphere, RH = right hemisphere.

2.2. Discriminant validity

To assess the degree to which the association of conscientiousness with network efficiency is specific to the SVAN, we repeated the permutation-selection approach using the parcels of the FPCN and the DN. The largest functional ensemble of the FPCN contained 7 parcels in the bilateral dorsolateral PFC and right anterior cingulate cortex that met the criteria from the permutation-selection procedure in Samples 1 and 2. For this network, efficiency values were computed from OMSTs-filtered graphs in the same manner as for the SVAN, using all parcels first and then all combinations of functional ensembles using the 7 parcels. We fit regression models predicting conscientiousness from efficiency of the full network, as well as efficiency of all combinations of functional ensembles from these 7 parcels, controlling for the effects of age, sex, intelligence, head motion, and efficiency of all parcels in the SVAN and DN.

This process was then repeated for the DN. The largest functional ensemble of the DN contained 43 parcels which met the criteria from the permutation-selection procedure in Samples 1 and 2. Considering the enormous number of possible combinations of parcels that could be calculated as functional ensembles from this large set of parcels, we limited our analyses to the efficiency values for the OMSTs-filtered graphs of the full network, the largest functional ensemble, and all combinations of 42, 41, and 40 parcels, in order to limit combinatorial explosion. Although this subset of combinations does not sample all combinations of functional ensembles of the DN, our approach yielded a number of tests roughly comparable to the number conducted for the SVAN, making it a reasonable comparison. Age, sex, intelligence, head motion and the efficiency of all parcels in the SVAN and FPCN were included as predictors. Parcels in the FPCN and DN used in the combinations of functional ensembles are reported in the supplementary material.

Associations between conscientiousness and the full networks and largest functional ensembles of the FPCN and DN are reported in Table 4.

Across all samples, conscientiousness was not significantly associated with the efficiency among all parcels of the FPCN. In Samples 1 and 2, conscientiousness was associated with efficiency among the parcels of the largest functional ensemble after controlling pFDR. Additionally, conscientiousness was significantly associated with the efficiency of 64 functional ensembles (64% of combinations) in Sample 1 after controlling pFDR, and the efficiency of all functional ensembles in Sample 2 after controlling pFDR. However, none of these associations were replicated in Sample 3, which is the crucial test because Sample 3 was not involved in selecting the parcels in the first place. In tests of DN efficiency, conscientiousness was not significantly associated with the effi-

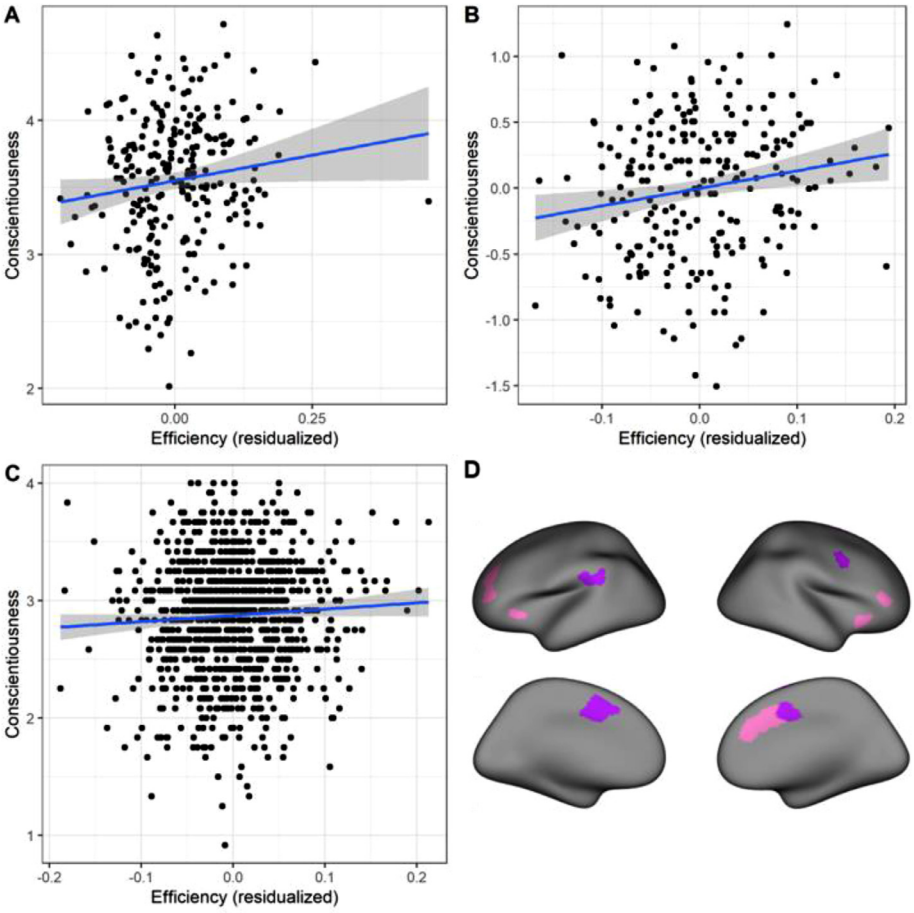

Fig. 3. Scatterplots of significant associations between efficiency of the largest functional ensemble of the SVAN with conscientiousness. **A** = Sample 1; **B** = Sample 2; **C** = Sample 3. Associations control for the effects of age, sex, intelligence, and efficiency of the frontoparietal control and default networks. The removal of the outlier on efficiency in Sample 1 altered the effect only slightly, and it remained significant (β = 0.29, q < 0.01). The effects also remained significant after the removal of high leverage points, identified as points with a leverage value greater than 2 times the number of parameters in the model divided by the sample size (Sample 1: β = 0.35, q < 0.01; Sample 2: β = 0.32, q < 0.01; Sample 3: β = 0.14, q < 0.01). **D** = parcels in the largest functional ensemble of the SVAN. SVAN = salience/ventral attention network. Purple = subnetwork A. Pink = subnetwork B.

Table 4
Standardized regression coefficients of models predicting conscientiousness from efficiency of whole networks and largest functional ensembles in FPCN and DN.

Model	Sample 1 (N = 244)		Sample 2 (N = 239)		Sample 3 (N = 1000)	
	All Parcels	Largest Functional Ensemble	All Parcels	Largest Functional Ensemble	All Parcels	Largest Functional Ensemble
Conscientiousness						
FPCN	.04	**.20***	−0.09	**.24****	−0.03	.04
Age	**.17**	**.17**	.07	.05	.04	.04
Sex (male)	**−0.45**	**−0.44**	**−0.55**	**−0.49**	**−0.17**	**−0.17**
Intelligence	**−0.14**	**−0.14**	.00	.01	**−0.10**	**−0.10**
Head motion	−0.06	−0.08	−0.04	−0.05	−0.06	−0.06
SVAN	−0.01	−0.06	−0.01	−0.17	.12	.09
DN	.00	−0.07	.15	.04	−0.14	**−0.17**
Conscientiousness						
DN	.00	.12	.15	**.39***	−0.14	−0.09
Age	**.17**	**.17**	.07	.07	.04	.04
Sex (male)	**−0.45**	**−0.42**	**−0.55**	**−0.53**	**−0.17**	**−0.16**
Intelligence	**−0.14**	**−0.14**	.00	−0.01	**−0.10**	**−0.10**
Head motion	−0.06	−0.06	−0.04	−0.05	−0.06	−0.06
SVAN	−0.01	−0.07	−0.01	−0.11	.12	.09
FPCN	.04	.00	−0.09	−0.20	−0.03	−0.05

Note. Associations with FPCN efficiency control for whole DN efficiency, and vice versa. Both regressions also control for whole SVAN efficiency. Estimates significant at uncorrected p < .05 shown in bold.

* q <0.05,

** q < 0.01 controlling across all combinations of functional ensembles (36 FPCN combinations and 13,288 DN combinations). FPCN = frontoparietal control network. DN = default network. Largest functional ensemble refers to the set of all parcels identified by the permutation selection procedure.

Table 5
Standardized regression coefficients of models predicting SVAN efficiency from the Big Five dimensions.

SVAN	C	E	A	N	O/I
Sample 1 (N = 244)					
All Parcels	−0.02	.03	−0.04	**−0.05***	.02
Largest Functional Ensemble	.05	.01	−0.03	**−0.07***	.00
Sample 2 (N = 239)					
All Parcels	.00	−0.02	−0.01	.01	.00
Largest Functional Ensemble	.01	−0.05	.00	.02	.02
Sample 3 (N = 1000)					
All Parcels	**.04***	.02	−0.02	.03	.01
Largest Functional Ensemble	**.04***	.03	−0.02	.02	.02

Note. Associations controlling for the age, sex, intelligence, head motion, and efficiency of the frontoparietal control and default networks. Estimates significant at uncorrected $p < .05$ shown in bold. SVAN = salience/ventral attention network. C = Conscientiousness, E = Extraversion, A = Agreeableness, N = Neuroticism, O/I = Openness/Intellect. Largest functional ensemble refers to the set of all parcels identified by the permutation selection procedure.

* q <0.05 controlling across all 16,278 combinations of functional ensembles.

ciency among all parcels of the DN in any sample after controlling pFDR. Conscientiousness was significantly associated with the efficiency of all functional ensembles in Sample 2 after controlling pFDR, but these associations were not replicated in Samples 1 and 3. The lack of replicable associations between conscientiousness and efficiency in the DN and FPCN provides evidence of discriminant validity, demonstrating that associations with the SVAN are probably not attributable to factors like network size or general characteristics of brain network integration.

To further assess discriminant validity, we conducted additional exploratory analyses to determine whether these associations with SVAN were exclusive to conscientiousness relative to the other Big Five dimensions. For each sample, we repeated our analyses including all Big Five traits as simultaneous predictors in models predicting efficiency of the full SVAN and combinations of functional ensembles. Standardized regression coefficients for each of the Big Five predicting efficiency of all parcels in the SVAN and the largest functional ensemble are reported in Table 5.

Among associations between traits other than conscientiousness, efficiency values of the full SVAN and its largest functional ensemble in Sample 1 were significantly negatively associated with neuroticism after controlling pFDR, but this association was not replicated in Samples 2 and 3. Interestingly, conscientiousness was not significantly associated with efficiency of the full SVAN or its largest functional ensemble in Samples 1 and 2 after controlling for the remaining Big Five and controlling pFDR, but conscientiousness in Sample 3 remained significantly positively associated with efficiency in the full SVAN and 14,330 functional ensembles (88% of all combinations), including the largest functional ensemble, after controlling for the remaining Big Five and controlling pFDR. Although this association between conscientiousness and efficiency of the SVAN was statistically significant only in Sample 3, the magnitude of the effect in Sample 1 is similar to that of Sample 3, suggesting the possibility that these results in Sample 1 may be indicative of Type II error as a result of lower statistical power in a smaller sample. Regardless, conscientiousness was the only trait among the Big Five to consistently exhibit positive associations with efficiency of the largest functional ensemble of the SVAN across samples, providing further evidence of discriminant validity.

3. Discussion

This research presents evidence of an association of conscientiousness with the functional connectivity of a set of parcels within the SVAN in three samples. These parcels, located in regions of medial and lateral PFC, insula, and parietal operculum, are widely dispersed throughout many nodes in both subnetworks of the SVAN identified by the 17-network atlas of Yeo et al. (2011). Considering the nature of our parcel selection procedure in constructing subsets of potentially relevant parcels, the magnitude of these associations may be overestimated in the first two samples. However, because the much larger third sample (HCP) did not contribute any parcels to this procedure, the significant effect in HCP is noteworthy as a fully independent and unbiased replication.

Additionally, in our supplementary material, we report results of analyses parallel to our main analyses but using negative correlations of conscientiousness with individual connections between parcels to identify sets of parcels in which to calculate network efficiency. This is an especially stringent test of our hypothesis. Regardless of the existence of a set of parcels in which efficiency is robustly positively associated with conscientiousness, if there were another set of parcels in which efficiency was negatively associated with conscientiousness, this would be contrary to our hypothesis. However, no set of parcels had efficiency that was consistently negatively associated with conscientiousness across samples.

The effects we report are small, but this should not be surprising given that participants were merely resting rather than being required to engage actively in some task involving goal prioritization. In personality neuroscience generally, we should expect the functional properties of networks to be more strongly associated with relevant traits when those networks are actively carrying out the psychological functions corresponding to the trait in question. The magnitude of the association between conscientiousness and the largest functional ensemble of the SVAN in Sample 3 is consistent with research on the range of effect sizes for associations between behavioral individual differences and resting brain function, making the large size of Sample 3 important for our ability to test this effect (Marek et al., 2022).

Associations between conscientiousness and the SVAN are consistent with previous research describing the network's functional roles. In its initial conception, the ventral attention network was largely right-lateralized and included the TPJ and regions of ventral PFC. It has been described as responsible for monitoring and redirecting attentional processes as a response to new and potentially salient cues from the environment (Corbetta and Shulman, 2002; Fox et al., 2006; Vossel et al., 2014). The salience network, typically described as consisting of the dorsomedial PFC, dACC, insula, and select regions of the dorsolateral PFC, has been attributed a similar function to the ventral attention network but with greater emphasis on the integration of information from a variety of sources to discern the relevance of incoming stimuli to one's motivation and goals (Menon and Uddin, 2010; Seeley et al., 2007; Uddin, 2015). Although previous research has sometimes characterized the ventral attention and salience networks as independent functional systems (Power et al., 2011; Cole et al., 2013; Baker et al., 2014), their anatomical and functional overlap has led to a growing consensus that they refer to a single large network with identifiable subnetworks (Uddin et al., 2019). Note, however, that the two subnetworks identified in the atlas of Yeo et al. (2011) and analyzed in this study do not correspond neatly to a distinction between the previously described ventral attention and salience networks.

The parcels in which efficiency was consistently associated with conscientiousness were spread across both SVAN subnetworks, suggesting that conscientious individuals may be characterized by effective integration of nodes relevant to all functions of the SVAN. This efficiency may permit a greater capability to identify and prioritize motivationally salient information in the context of multiple goals of varying duration, importance, and abstraction. These findings also have important implications in the context of evidence supporting the involvement of the SVAN in modulating the activity of the DN and FPCN (Bonnelle et al., 2012; Kucyi et al., 2017; Zhou et al., 2018). Through this interpretation, our results suggest that individual differences in conscientiousness may be partially contingent on differences in the adeptness of the SVAN in

managing the dynamic tension between these two networks. This particular role of the SVAN coheres well with the notion of goal prioritization as coordinating internal representations of various goal states (DN) with information in working memory (FPCN) used to monitor progress toward these goals and direct ongoing action related to them.

Further, this interpretation is consistent with much of the literature describing the functional and structural properties of regions where the parcels in question are located, particularly the dorsolateral PFC, insula, and dorsomedial PFC. Previous literature has described associations of functional connectivity among these regions with a variety of higher-order self-regulatory processes conceptually related to conscientiousness (Cieslik et al., 2013; Lynn et al., 2014; Taren et al., 2011). Several structural MRI studies have found conscientiousness to be associated with structural variables such as cortical thickness in regions of dorsolateral PFC corresponding reasonably well to particular parcels identified in the present research (Bjørnebekk et al., 2013; Gao et al., 2021; Owens et al., 2019). These regions of the dorsolateral PFC may be particularly responsible for maintaining the representations that regulate the pursuit of active goals and suppress distractions arising from salient information identified through other SVAN regions such as the insula (Dosenbach et al., 2008; Rueter et al., 2018). Thus, our results describe replicable associations of conscientiousness with functional integration in the SVAN in a manner that seems consonant with previous literature describing the neural correlates of well-regulated goal pursuit.

Our findings also serve as an important clarification and extension of findings by Rueter et al. (2018), supporting the theory that the SVAN is a key neurological substrate of individual differences in conscientiousness. However, our methods allowed us to make a more precise and generalizable test of the hypothesis that functional connectivity in the SVAN is positively associated with conscientiousness. Because Rueter et al. (2018) relied on ICA to identify intrinsic connectivity networks that overlapped with the SVAN more than with other canonical networks, the boundaries of the networks identified by ICA did not correspond particularly well to the SVAN's boundaries. In our supplementary materials, we report analyses in which we tried to replicate, as closely as possible using our parcellation, the spatial extent of ICA networks that Rueter et al. (2018) found to be associated with conscientiousness. The efficiency of this set of parcels was not replicable in our other samples.

Additionally, to investigate the effect of using individualized parcels in our study, we repeated our analyses using measures of network efficiency of the SVAN derived from non-individualized parcels of the standard group-level atlas across all three samples. Consistent with previous research on the effects of individualized parcellation, we found that the majority of associations of conscientiousness with network efficiency of the SVAN, its subnetworks, and combinations of functional ensembles were greater when using individualized parcels than when using the standard atlas. These results are described in detail in the supplementary materials.

The present research incorporates many practices that have been shown in recent work to improve test-retest reliability among resting-state fMRI findings, including the use of individualized cortical parcellation (Chong et al., 2017), the Schaefer atlas (Schaefer et al., 2018), weighted graphs determined by product-moment correlations, and graph filtering through OMSTs (Luppi et al., 2021; Luppi and Stamatakis, 2021). Specifically, using OMSTs to assess functional connectivity allowed us to capture meaningful individual variability in functional topology among parcels by modeling associations among them in a manner that maximizes global-cost efficiency, consequently bypassing both the need to impose an arbitrary threshold and the retention of excess noise in graph theoretical measures. By simultaneously modeling efficient information transfer and sparsity using OMSTs, our approach effectively characterizes brain connectivity as high-performing and adaptable small-world networks with modular and hierarchical properties, which corresponds well to what is known about actual brain function (Bassett and Bullmore, 2006; Mengistu et al., 2016).

3.1. Limitations

Despite the advantages of our methods, there are limitations to consider regarding the current research. Although we identified a set of parcels for which associations with conscientiousness were replicable in a large, independent sample, we also saw some variability across samples in associations between conscientiousness and the efficiency of various networks and functional ensembles. This variability could be related to variability in participant characteristics, scanning parameters, and/or personality measures. For example, measurement quality might help explain why Sample 1, with multiple self- and peer-report measures of personality, demonstrated stronger associations between neural variables and conscientiousness than Sample 3, which had only a single, relatively brief, self-report measure of personality.

Additionally, the permutation-based parcel selection procedure used to identify subnetworks for each of the canonical networks of interest used a cutoff of parcels appearing in 80% of iterations. This cutoff was chosen to permit a suitably sized pool of candidate parcels while also affording manageable computational intensity during the calculation of functional ensemble combinations. This somewhat arbitrary threshold defined the size of the largest functional ensemble for each network, and a different threshold might have yielded different results. As a robustness check, we repeated our main analyses using a cutoff of 70% and found that our results did not change substantively. Additionally, a cutoff of 90% produced similar results for the entire SVAN, but yielded too few candidate parcels (<3) for subnetworks A and B. Our analyses were also restricted to investigating the efficiency of the SVAN, FPCN, and DN. It is possible that other, less obviously relevant networks could be related to conscientiousness. It is also possible that connectivity between networks is relevant, whereas we limited our investigation to connectivity within networks. Future research could address these possibilities.

4. Conclusion

Using resting-state fMRI, in conjunction with canonical networks of individualized parcels and graph theoretical measures, we identified a set of regions in the SVAN, including nodes in the anterior insula, dorsolateral PFC, parietal operculum, and dACC, in which network efficiency was a replicable neural correlate of conscientiousness across three samples. These results are consistent with a theory that the ability to prioritize goals effectively underlies conscientiousness and relies primarily on the SVAN (Allen and DeYoung, 2017; Rueter et al., 2018). Our findings emphasize the importance of several existing and emerging practices in personality neuroscience (DeYoung et al., 2022), including the use of theory-driven analyses and large sample sizes, and individualized parcellation to capture variability in the cortical location of canonical neural networks. Although this is basic research, it may eventually contribute to the development of novel interventions for mental health problems involving impulsivity and disinhibition, the dimension of psychopathology corresponding to maladaptive low conscientiousness.

Data/Code availability

Individual data from Sample 1 are not able to be shared through open access because participants agreed during the informed consent procedure that their data would not be shared beyond the research team. Data from Sample 3 are available from the Human Connectome Project's website: https://www.humanconnectome.org/study/hcp-young-adult. A sample-average functional connectivity matrix from Sample 1 using individualized parcels, as well as individualized functional connectivity matrices from Sample 2 are available in an Open Science Framework repository: https://osf.io/zju2s/?view_only=8521207b2af540b9bab3b04033744f39. This repository also contains scripts used in group-level analyses. Code used to produce individualized parcels is available at https://neuroimageusc.github.io/GPIP

Declaration of Competing Interest

None.

Credit authorship contribution statement

Tyler A. Sassenberg: Methodology, Software, Validation, Formal analysis, Investigation, Writing – original draft, Writing – review & editing, Visualization, Project administration. **Philip C. Burton:** Software, Writing – review & editing, Visualization. **Laetitia Mwilambwe-Tshilobo:** Software, Data curation, Writing – review & editing. **Rex E. Jung:** Resources, Data curation, Writing – review & editing, Funding acquisition. **Aldo Rustichini:** Writing – review & editing, Funding acquisition. **R. Nathan Spreng:** Software, Resources, Data curation, Writing – review & editing. **Colin G. DeYoung:** Conceptualization, Methodology, Writing – original draft, Writing – review & editing, Supervision, Funding acquisition.

Data availability

The link to available data is found in the data/code availability statement

Acknowledgments

We would like to thank Amanda Rueter, Katherine Scotting, and Ranee Flores for their feedback and input in this work. Data collection was supported by grants from the National Institute on Drug Abuse (R03DA029177-01A1) and the National Science Foundation (SES-1061817) to Colin DeYoung and Aldo Rustichini, and from the John Templeton Foundation (22156) to Rex Jung. We also thank the collectors and curators of the data from the Human Connectome Project.

Supplementary materials

Supplementary material associated with this article can be found, in the online version, at doi:10.1016/j.neuroimage.2023.120081.

References

Allen, T.A., DeYoung, C.G., Widiger, T.A., 2017. Personality neuroscience and the Five Factor Model. In: Oxford Handbook of the Five Factor Model. Oxford University Press, New York, pp. 319–349.

Anderson, K.M., Ge, T., Kong, R., Patrick, L.M., Spreng, R.N., Sabuncu, M.R., Yeo, B.T.T., Holmes, A.J., 2021. Heritability of individualized cortical network topography. Proc. Natl. Acad. Sci. 118 (9), e2016271118. doi:10.1073/pnas.2016271118.

Baker, J.T., Holmes, A.J., Masters, G.A., Yeo, B.T.T., Krienen, F., Buckner, R.L., Öngür, D., 2014. Disruption of cortical association networks in schizophrenia and psychotic bipolar disorder. JAMA Psychiatry 71 (2), 109–118. doi:10.1001/jamapsychiatry.2013.3469.

Bassett, D.S., Bullmore, E.T., 2006. Small-world brain networks. Neuroscientist 12, 512–523. doi:10.1177/1073858406293182.

Bjørnebekk, A., Fjell, A.M., Walhovd, K.B., Grydeland, H., Torgersen, S., Westlye, L.T., 2013. Neuronal correlates of the five factor model (FFM) of human personality: multimodal imaging in a large healthy sample. Neuroimage 65, 194–208. doi:10.1016/j.neuroimage.2012.10.009.

Bonnelle, V., Ham, T.E., Leech, R., Kinnunen, K.M., Mehta, M.A., Greenwood, R.J., Sharp, D.J., 2012. Salience network integrity predicts default mode network function after traumatic brain injury. Proc. Natl. Acad. Sci. 109 (12), 4690–4695. doi:10.1073/pnas.1113455109.

Bullmore, E., Sporns, O., 2012. The economy of brain network organization. Nat. Rev. Neurosci. 13 (5), 336–349. doi:10.1038/nrn3214.

Burgess, G.C., Kandala, S., Nolan, D., Laumann, T.O., Power, J.D., Adeyemo, B., Harms, M.P., Petersen, S.E., Barch, D.M, 2016. Evaluation of denoising strategies to address motion-correlated artifacts in resting-state functional magnetic resonance imaging data from the Human Connectome Project. Brain Connect. 6 (9), 669–680. doi:10.1089/brain.2016.0435.

Chong, M., Bhushan, C., Joshi, A.A., Choi, S., Haldar, J.P., Shattuck, D.W., Spreng, R.N., Leahy, R.M., 2017. Individual parcellation of resting fMRI with a group functional connectivity prior. Neuroimage 156, 87–100. doi:10.1016/j.neuroimage.2017.04.054.

Cieslik, E.C., Zilles, K., Caspers, S., Roski, C., Kellermann, T.S., Jakobs, O., Langner, R., Laird, A.R., Fox, P.T., Eickhoff, S.B., 2013. Is there "one" DLPFC in cognitive action control? Evidence for heterogeneity from co-activation-based parcellation. Cerebral Cortex 23, 2677–2689. doi:10.1093/cercor/bhs256.

Cole, M.W., Reynolds, J.R., Power, J.D., Repovs, G., Anticevic, A., Braver, T.S., 2013. Multi-task connectivity reveals flexible hubs for adaptive task control. Nat. Neurosci. 16 (9), 1348–1355. doi:10.1038/nn.3470.

Cole, M.W., Yarkoni, T., Repovš, G., Anticevic, A., Braver, T.S., 2012. Global connectivity of prefrontal cortex predicts cognitive control and intelligence. J. Neurosci. 32 (26), 8988–8999. doi:10.1523/JNEUROSCI.0536-12.2012.

Corbetta, M., Shulman, G.L., 2002. Control of goal-directed and stimulus-driven attention in the brain. Nat. Rev. 3, 201–215. doi:10.1038/nrn755.

Costa, P.T., McCrae, R.R., 1992. Revised NEO Personality Inventory (NEO PI-R) and NEO Five-Factor Inventory (NEOFFI) professional manual. Odessa, FL, Psychological Assessment Resources.

Dale, A.M., Fischl, B., Sereno, M.I., 1999. Cortical surface-based analysis: I. Segmentation and surface reconstruction. Neuroimage 9 (2), 179–194. doi:10.1006/nimg.1998.0395.

Deuker, L., Bullmore, E.T., Smith, M., Christensen, S., Nathan, P.J., Rockstroh, B., Bassett, D.S., 2009. Reproducibility of graph metrics of human brain functional networks. Neuroimage 47, 1460–1468. doi:10.1016/j.neuroimage.2009.05.035.

DeYoung, C.G., 2015. Cybernetic big five theory. J. Res. Pers. 56, 33–58. doi:10.1016/j.jrp.2014.07.004.

DeYoung, C.G., Beaty, R.E., Genç, E., Latzman, R.D., Passamonti, L., Servaas, M.N., Shackman, A.J., Smillie, L.D., Spreng, R.N., Viding, E., Wacker, J., 2022. Personality neuroscience: an emerging field with bright prospects. Pers. Sci. 3, 1–21. doi:10.5964/ps.7269.

DeYoung, C.G., Grazioplene, R.G., Allen, T.A, John, O.P., Robbins, R.W., 2021. The neurobiology of personality. Handbook of personality: Theory and research, Fourth Edition. Guilord Press, New York.

DeYoung, C.G., Quilty, L.C., Peterson, J.B., 2007. Between facets and domains: 10 aspects of the Big Five. J. Pers. Soc. Psychol. 93, 880–896. doi:10.1037/0022-3514.93.5.880.

Dimitriadis, S.I., Salis, C., Tarnanas, I., Linden, D.E., 2017. Topological filtering of dynamic functional brain networks unfolds informative chronnectomics: a novel data-driven thresholding scheme based on orthogonal minimum spanning trees (OMSTs). Front. Neuroinform. 11, 28. doi:10.3389/fninf.2017.00028.

Dosenbach, N.U.F., Fair, D.A., Cohen, A.L., Schlaggar, B.L., Petersen, S.E., 2008. A dual-networks architecture of top-down control. Trends Cogn. Sci. (Regul. Ed.) 12 (3), 99–105. doi:10.1016/j.tics.2008.01.001.

Dosenbach, N.U.F., Fair, D.A., Miezin, F.M., Cohen, A.L., Wenger, K.K., Dosenbach, R.A.T., Fox, M.D., Snyder, A.Z., Vincent, J.L., Raichle, M.E., Schlaggar, B.L., Petersen, S.E., 2007. Distinct brain networks for adaptive and stable task control in humans. Proc. Natl. Acad. Sci. 104 (26), 11073–11078. doi:10.1073/pnas.07043201014.

Esteban, O., Markiewicz, C., Blair, R.W., Moodie, C., Isik, A.I., Aliaga, A.E., Kent, J., et al., 2018. fMRIPrep: a robust preprocessing pipeline for functional MRI. Nat. Methods doi:10.1038/s41592-018-0235-4.

Finn, E.S., Shen, X., Scheinost, D., Rosenberg, M.D., Huang, J., Chun, M.M., Papademetris, X., Constable, R.T, 2015. Functional connectome fingerprinting: identifying individuals using patterns of brain connectivity. Nat. Neurosci. 18 (11), 1664–1671. doi:10.1038/nn.4135.

Fox, M.D., Corbetta, M., Snyder, A.Z., Vincent, J.L., Raichle, M.E, 2006. Spontaneous neuronal activity distinguishes human dorsal and ventral attention systems. PNAS 103 (26), 10046–10051. doi:10.1073/pnas.0604187103.

Gao, K., Zhang, R., Xu, T., Zhou, F., Feng, T., 2021. The effect of conscientiousness on procrastination: the interaction between the self-control and motivation neural pathways. Hum. Brain Mapp. 42, 1829–1844. doi:10.1002/hbm.25333.

Glasser, M.F., Sotiropoulos, S.N., Wilson, J.A., Coalson, T.S., Fischl, B., Andersson, J.L., Xu, J., Jbabdi, S., Webster, M., Polimeni, J.R., Van Essen, D.C., … Jenkinson, M.WU-Minn HCP Consortium, 2013. The minimal preprocessing pipelines for the human connectome project. Neuroimage 80, 105–124. doi:10.1016/j.neuroimage.2013.04.127.

Gordon, E.M., Laumann, T.O., Adeyemo, B., Petersen, S.E., 2017. Individual variability of the system-level organization of the human brain. Cerebral Cortex 27 (1), 386–399. doi:10.1093/cercor/bhv239.

Heaton, R.K., Akshoomoff, N., Tulsky, D., Mungas, D., Weintraub, S., Dikmen, S., Beaumont, J., Casaletto, K.B., Conway, K., Slotkin, J., Gershon, R, 2014. Reliability and validity of composite scores from the NIH toolbox cognitive battery in adults. J. Int. Neuropsychol. Soc. 20 (6), 588–598. doi:10.1017/S1355617714000241.

Higgins, D.M., Peterson, J.B., Pihl, R.O., Lee, A.G.M., 2007. Prefrontal cognitive ability, intelligence, big five personality, and the prediction of advanced academic and workplace performance. J. Pers. Soc. Psychol. 93 (2), 298–319. doi:10.1037/0022-3514.93.2.298.

Jiang, C., He, Y., Betzel, R.F., Wang, Y.-S., Xing, X.-X., Zuo, X.-N., 2021. Optimizing network neuroscience computation of individual differences in human spontaneous brain activity for test-retest reliability. bioArXiv doi:10.1101/2021.05.06.442886.

John, O.P., Naumann, L.P., Soto, C.J., John, O.P., Robins, R.W., Pervin, L.A., 2008. Paradigm shift to the integrative big-five trait taxonomy: history, measurement, and conceptual issues. In: Handbook of Personality: Theory and Research. Guilford Press, New York, NY, pp. 114–158.

Kong, R., Li, J., Orban, C., Sabuncu, M.R., Liu, H., Schaefer, A., Sun, N., Zuo, X.N., Holmes, A.J., Eickhoff, S.B., Yeo, B.T.T, 2018. Spatial topography of individual-specific cortical networks predicts human cognition, personality, and emotion. Cerebral Cortex 29 (6), 1–19. doi:10.1093/cercor/bhy123.

Kong, R., Yang, Q., Gordon, E., Xue, A., Yan, X., Orban, C., Zuo, X., Spreng, R.N., Ge, T., Holmes, A., Eickhoff, S., Yeo, B.T.T., 2021. Individual-specific areal-level parcellations improve functional connectivity prediction of behavior. Cerebral Cortex 31 (10), 4477–4500. doi:10.1093/cercor/bhab101.

Kucyi, A., Hove, M.J., Esterman, M., Hutchison, R.M., Valera, E.M., 2017. Dynamic brain network correlates of spontaneous fluctuations in attention. Cerebral Cortex 27 (3), 1831–1840. doi:10.1093/cercor/bhw029.

Luppi, A.I., Gellersen, H.M., Peattie, A.R.D., Manktelow, A.E., Menon, D.K., Dimitriadis, S.I., Stamatakis, E.A., 2021. Searching for consistent brain network topologies across the garden of (shortest) forking paths. bioArXiv doi:10.1101/2021.07.13.452257.

Luppi, A.I., Stamatakis, E.A., 2021. Combining network topology and information theory to construct representative brain networks. Netw. Neurosci. 5 (1), 96–124. doi:10.1162/netn_a_00170.

Lynn, M.T., Muhle-Karbe, P.S., Brass, M., 2014. Controlling the self: the role of the dorsal frontomedian cortex in intentional inhibition. Neuropsychologia 65, 247–254. doi:10.1016/j.neuropsychologia.2014.09.009.

Marek, S., Tervo-Clemmens, B., Calabro, F.J., et al., 2022. Reproducible brain-wide association studies require thousands of individuals. Nature 603, 654–660. doi:10.1038/s41586-022-04492-9.

Mengistu, H., Huizinga, J., Mouret, J.B., Clune, J., 2016. The evolutionary origins of hierarchy. PLOS Comput. Biol. 12, e1004829. doi:10.1371/journal.pcbi.1004829.

Menon, V., Uddin, L.Q., 2010. Saliency, switching, attention and control: a network model of insula function. Brain Struct. Funct. 214 (5), 655–667. doi:10.1007/s00429-010-0262-0.

Moore, T.M., Reise, S.P., Gur, R.E., Hakonarson, H., Gur, R.C., 2015. Psychometric properties of the penn computerized neurocognitive battery. Neuropsychology 29 (2), 235–246. doi:10.1037/neu0000093.

Ozer, D.J., Benet-Martinez, V., 2006. Personality and the prediction of consequential outcomes. Annu. Rev. Psychol. 57, 401–421. doi:10.1146/annurev.psych.57.102904.190127.

Owens, M.M., Hyatt, C.S., Gray, J.C., Carter, N.T., MacKillop, J., Miller, J.D., Sweet, L.H., 2019. Cortical morphometry of the five-factor model of personality: findings from the human connectome project full sample. Soc. Cogn. Affect. Neurosci. 14 (4), 381–395. doi:10.1093/scan/nsz017.

Power, J.D., Barnes, K.A., Snyder, A.Z., Schlaggar, B.L., Petersen, S.E., 2012. Spurious but systematic correlations in functional connectivity MRI networks arise from subject motion. Neuroimage 59 (3), 2142–2154. doi:10.1016/j.neuroimage.2011.10.018.

Power, J.D., Cohen, A.L., Nelson, S.M., Wig, G.S., Barnes, K.A., Church, J.A., Vogel, A.C., Laumann, T.O., Miezin, F.M., Schlaggar, B.L., Petersen, S.E., 2011. Functional network organization of the human brain. Neuron 72 (4), 665–678. doi:10.1016/j.neuron.2011.09.006.

Power, J.D., Mitra, A., Laumann, T.O., Snyder, A.Z., Schlaggar, B.L., Petersen, S.E., 2014. Methods to detect, characterize, and remove motion artifact in resting state fMRI. Neuroimage 84 (Supplement C), 320–341. doi:10.1016/j.neuroimage.2013.08.048.

Roberts, B.W., Lejuez, C., Krueger, R.F., Richards, J.M., Hill, P.L., 2014. What is conscientiousness and how can it be assessed? Dev. Psychol. 50 (5), 1315–1330. doi:10.1037/a0031109.

Rosenberg, M.D., Finn, E.S., Scheinost, D., Papademetris, X., Shen, X., Constable, R.T., Chun, M.M., 2015. A neuromarker of sustained attention from whole-brain functional connectivity. Nat. Neurosci. 19 (1), 165–171. doi:10.1038/nn.4179.

Rubinov, M., Sporns, O., 2010. Complex network measures of brain connectivity: uses and interpretations. Neuroimage 52, 1059–1069. doi:10.1016/j.neuroimage.2009.10.003.

Rueter, A.R., Abram, S.V., MacDonald III, A.W., Rustichini, A., DeYoung, C.G, 2018. The goal priority network as a neural substrate of conscientiousness. Hum. Brain Mapp. 39 (9), 3574–3585. doi:10.1002/hbm.24195.

Schaefer, A., Kong, R., Gordon, E.M., Laumann, T.O., Zuo, X.N., Holmes, A.J., Eickhoff, S.B., Yeo, B.T.T, 2018. Local-global parcellation of the human cerebral cortex from intrinsic functional connectivity MRI. Cerebral Cortex 28, 3095–3114. doi:10.1093/cercor/bhx179.

Seeley, W.W., Menon, V., Schatzberg, A.F., Keller, J., Glover, G.H., Kenna, H., Reiss, A.L., Greicius, M.D., 2007. Dissociable intrinsic connectivity networks for salience processing and executive control. J. Neurosci. 27 (9), 2349–2356. doi:10.1523/JNEUROSCI.5587-06.2007.

Setton, R., Mwilambwe-Tshilobo, L., Sheldon, S., Turner, G.R., Spreng, R.N., 2022. Hippocampus and temporal pole functional connectivity is associated with age and individual differences in autobiographical memory. Proc. Natl. Acad. Sci. 119, e2203039119. doi:10.1073/pnas.2203039119.

Setton, R., Mwilambwe-Tshilobo, L., Girn, M., Lockrow, A.W., Baracchini, G., Hughes, C., Lowe, A.J., Cassidy, B.N., Li, J., Luh, W., Bzdok, D., Leahy, R.M., Ge, T., Margulies, D.S., Misic, B., Bernhardt, B.C., Stevens, W.D., De Brigard, F., Kundu, P., Turner, G.R., Spreng, R.N., 2023. Age differences in the functional architecture of the human brain. Cerebral Cortex 33 (1), 114–134. doi:10.1093/cercor/bhac056.

Shen, X., Finn, E.S., Scheinost, D., Rosenberg, M.D., Chun, M.M., Papademetris, X., Constable, R.T., 2017. Using connectome-based predictive modeling to predict individual behavior from brain connectivity. Nat. Protoc. 12 (3), 506–518. doi:10.1038/nprot.2016.178.

Storey, J.D., 2002. A direct approach to false discovery rates. J. R. Stat. Soc. Ser. B (Stat. Methodol.) 64 (3), 479–498. doi:10.1111/1467-9868.00346.

Storey, J.D., 2003. The positive false discovery rate: a Bayesian interpretation of the q-value. Ann. Statist. 31 (6), 2013–2035. https://www.jstor.org/stable/3448445.

Storey, J.D., Tibshirani, R., 2003. Statistical significance for genomewide studies. PNAS 100 (16), 9440–9445. doi:10.1073/pnas.1530509100.

Taren, A.A., Venkatraman, V., Huettel, S.A., 2011. A parallel functional topography between medial and lateral prefrontal cortex: evidence and implications for cognitive control. J. Neurosci. 31 (13), 5026–5031. doi:10.1523/JNEUROSCI.5762-10.2011.

Tewarie, P., van Dellen, E., Hillebrand, A., Stam, C.J., 2015. The minimum spanning tree: an unbiased method for brain network analysis. Neuroimage 104, 177–188. doi:10.1016/j.neuroimage.2014.10.015.

Uddin, L.Q., 2015. Salience processing and insular cortical function and dysfunction. Nat. Rev. Neurosci. 16 (1), 55–61. doi:10.1038/nrn3857.

Uddin, L.Q., Yeo, B.T.T., Spreng, R.N., 2019. Towards a universal taxonomy of macro-scale functional human brain networks. Brain Topogr. 32 (6), 926–942. doi:10.1007/s10548-019-00744-6.

Ugurbil, K., Xu, J., Auerbach, E.J., Moeller, S., Vu, A.T., Duarte-Carvajalino, J.M., Lenglet, C., Wu, X., Schmitter, S., Van de Moortele, P.F., Strupp, J., Sapiro, G., De Martino, F., Wang, D., Harel, N., Garwood, M., Chen, L., Feinberg, D.A., … Yacoub, E., 2013. Pushing spatial and temporal resolution for functional and diffusion MRI in the Human Connectome Project. Neuroimage 80, 80–104. doi:10.1016/j.neuroimage.2013.05.012.

Van Essen, D.C., Smith, S.M., Barch, D.M., Behrens, T.E.J., Yacoub, E., Ugurbil, K.WU-Minn HCP Consortium, 2013. The WU-Minn human connectome project: an overview. Neuroimage 80, 62–79. doi:10.1016/j.neuroimage.2013.05.041.

Van Essen, D., Ugurbil, K., Auerbach, E., Barch, D., Behrens, T., Bucholz, R., Chang, A., Chen, L., Corbetta, M., Curtiss, S., Penna, D., Feinberg, D., Glasser, M.F., Harel, N., Heath, A.C., Larson-Prior, L., Marcus, D., Michalareas, G., Moeller, S., … Oostenveld, R.WU-Minn Consortium, 2012. The Human Connectome Project: a data acquisition perspective. Neuroimage 62 (4), 2222–2231. doi:10.1016/j.neuroimage.2012.02.018.

Vossel, S., Geng, J.J., Fink, G.R., 2014. Dorsal and ventral attention systems: distinct neural circuits but collaborate roles. The Neurosci. 20 (2), 150–159. doi:10.1177/1073858413494269.

Wang, Z., Goerlich, K.S., Ai, H., Aleman, A., Luo, Y., Xu, P., 2021. Connectome-based predictive modeling of individual anxiety. Cerebral Cortex 31 (6), 3006–3020. doi:10.1093/cercor/bhaa407.

Wechsler, D., 2008. WAIS-IV Administration and Scoring Manual. Pearson.

Wechsler, D., 2011. WASI-II: Wechsler abbreviated Scale of Intelligence. PsychCorp.

Widiger, T.A., Sellbom, M., Chmielewski, M., Clark, L.A., DeYoung, C.G., Kotov, R., Krueger, R.F, Lynam, D.R., Miller, J.D., Mullins-Sweatt, S., Samuel, D.B., South, S.C., Tackett, J.L., Thomas, K.M., Watson, D., Wright, A.G.C., 2019. Personality in a hierarchical model of psychopathology. Clin. Psychol. Sci. 7, 77–92. doi:10.1177/2167702618797105.

Wilmot, M.P., Ones, D.S., 2019. A century of research on Conscientiousness at work. PNAS 116 (46), 23004–23010. doi:10.1073/pnas.1908430116.

Yeo, B.T.T., Krienen, F.M., Sepulcre, J., Sabuncu, M.R., Lashkari, D., Hollinshead, M., Roffman, J.L., Smoller, J.W., Zöllei, L., Polimeni, J.R., Fischl, B., Liu, H., Buckner, R.L., 2011. The organization of the human cerebral cortex estimated by intrinsic functional connectivity. J. Neurophysiol. 106 (3), 1125–1165. doi:10.1152/jn.00338.2011.

Zhou, Y., Friston, K.J., Zeidman, P., Chen, J., Li, S., Razi, A., 2018. The hierarchical organization of the default, dorsal attention and salience networks in adolescents and young adults. Cerebral Cortex 28, 726–737. doi:10.1093/cercor/bhx307.